ACS APPLIED MATERIALS & INTERFACES

Letter

www.acsami.org

Hybrid MnO_2 Film with Agarose Gel for Enhancing the Structural Integrity of Thin Film Supercapacitor Electrodes

Soomin Park,[†] Inho Nam,[†] Gil-Pyo Kim,[†] Jeong Woo Han,[‡] and Jongheop Yi*[,†]

[†]World Class University (WCU) program of Chemical Convergence for Energy & Environment (C2E2), Institute of Chemical Processes, School of Chemical and Biological Engineering, College of Engineering, Seoul National University, Seoul, 151-742, Republic of Korea

[‡]Department of Chemical Engineering, University of Seoul, Seoul, 130-743, Republic of Korea

Supporting Information

ABSTRACT: We report on the fabrication of a robust hybrid film containing MnO_2 for achieving large areal capacitances. An agarose gel, as an ion-permeable and elastic layer coated on a current collector, plays a key role in stabilizing the deposited pseudocapacitive MnO_2. Cyclic voltammetry and electrochemical impedance spectroscopy data indicate that the hybrid electrode is capable of exhibiting a high areal capacitance up to 52.55 mF cm^{-2}, with its superior structural integrity and adhesiveness to the current collector being maintained, even at a high MnO_2 loading.

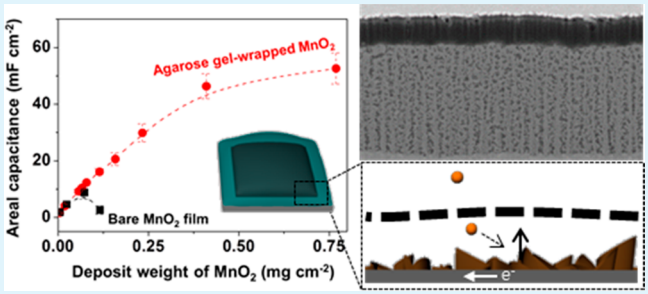

KEYWORDS: *supercapacitor, electrochemistry, agarose gel, manganese oxide, areal capacitance*

1. INTRODUCTION

Many attempts have been made to improve the energy/power density of energy storage systems (ESS) by introducing thin film architectures to electrode materials. Certain types of thin film electrode materials reported show low ion diffusion length and reduced electron transfer resistance that are related to the major properties of the next generation ESS.[1−5] Until now, however, there are problems associated with thin film electrodes, including a short life cycle and limitations in thickness. More importantly, the development of film-type electrodes that are capable of storing more energy per unit area has become an urgent issue in order to meet future demands of the electronics industry.

One of the fatal problems for the practical use is the fragile characteristics of thin film-type materials. As an example, anodic/cathodic electrodeposition is one of the most controllable approaches for the fabrication of thin film electrodes.[6,7] In this method, it is possible to precisely control the film thickness and morphology of active materials.[8−11] Nevertheless, disintegration of the deposited layer results in contact failure between the active material film and the current collector. This is closely related to the fading in the performance of energy storage devices.[12,13] This characteristic is common across all techniques associated with thin film fabrication and it is highly dependent on the adhesion and thickness of the active layer as well as the formation of cracks in the deposited films.

To find a solution to these issues, we report herein on the synthesis of a robust metal oxide thin film by agarose gel wrapping. We coated an agarose gel on a metallic current collector prior to the electrodeposition of an active metal oxide. Agarose gels are comprised of a polymer matrix with submicrometer pores (pore sizes of 400−500 nm) and high elasticity (Young's modulus of 116 kPa).[14,15] Such hydrogels show, not only great film-forming ability on a substrate during the sol−gel process but also have a high accessibility for an ionic metal precursor and an electrolyte in aqueous solution.[16−18]

Our proof-of-concept research is based on the preparation of manganese dioxide (MnO_2) films for use in supercapacitor applications. As a pseudocapacitive electrode material, MnO_2 has attracted considerable interest because of its properties that include a high theoretical specific capacitance (1370 F g^{-1}), low cost, and the fact that it is environmentally benign.[7,19] However, the major problem associated with MnO_2 is the high charge-transfer resistance between the MnO_2 film and the metallic current collector, which can be attributed to the low adhesion of such films.[7] In addition, in the case when the amount of MnO_2 deposited is increased, film contact to the current collector becomes deteriorated because of film shrinkage during the oxidation of Mn hydroxide.[12,13] Therefore, an upper limit exists for capacitance per unit area of the current collector. For this reason, an electrodeposited MnO_2 film was selected as a representative model material to prove the effect of agarose gel hybridization.

In this study, we evaluated the electrochemical performance and morphology of an agarose gel-wrapped MnO_2 architecture. We also performed 3D finite element (FEM) simulations and the first-principles calculations to verify the superior elastic

Received: August 22, 2013
Accepted: September 30, 2013
Published: September 30, 2013

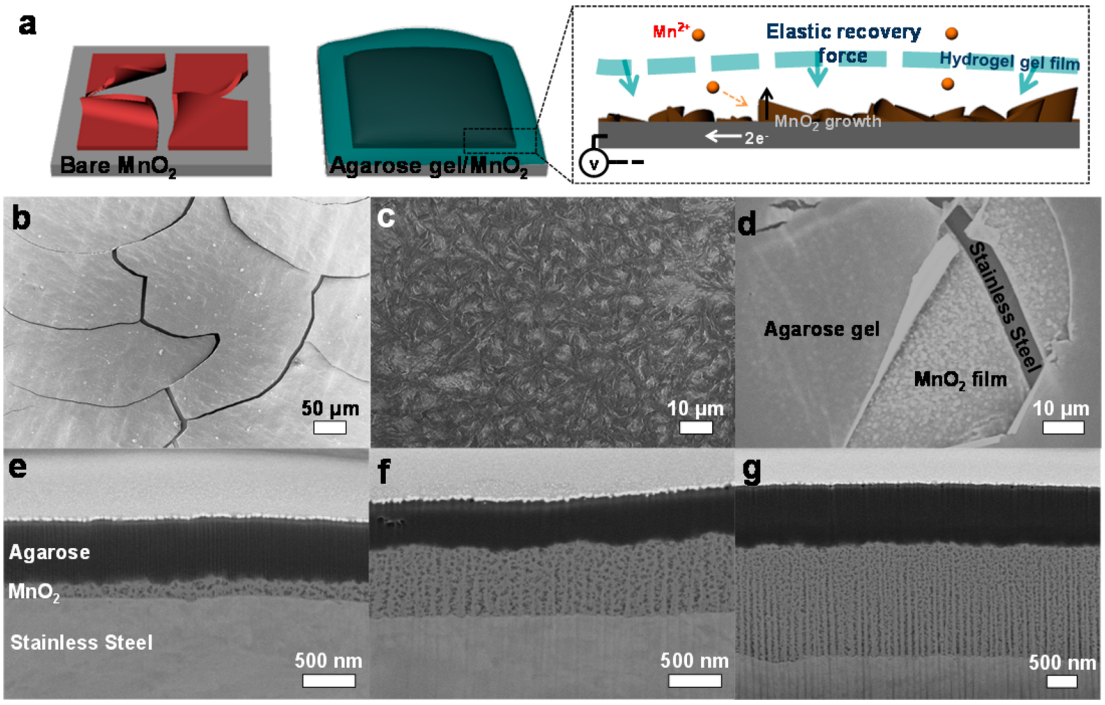

Figure 1. (a) Schematic illustration of agarose gel-wrapped MnO_2 film. (b) SEM images of the bare MnO_2 films, and SEM images of (c, d) top views and (e–g) side views of the agarose gel-wrapped MnO_2 films. Deposition amounts of MnO_2 are (b–d) 0.300 mg cm^{-2}, (e) 0.057 mg cm^{-2}, (f) 0.168 mg cm^{-2} and (g) 0.361 mg cm^{-2}, respectively.

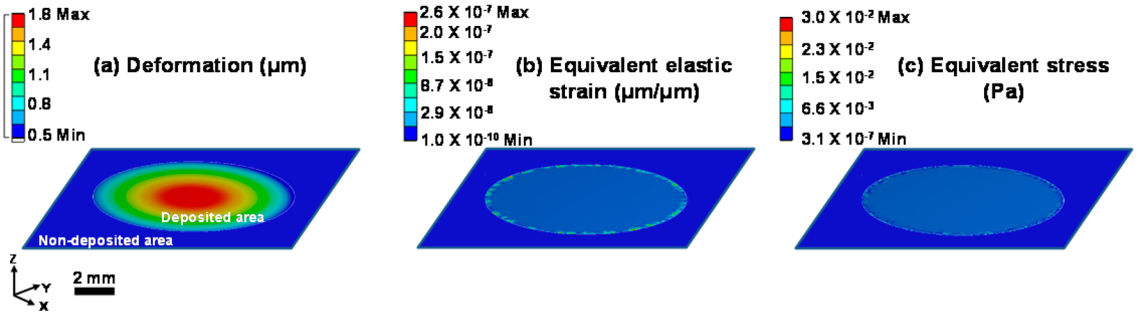

Figure 2. 3D FEM results. Deformation analyses (a) under high MnO_2 loading condition (maximum 1.8 μm depth), the calculated equivalent (b) elastic strain and (c) stress.

properties and ion accessibility of the agarose gel layer, respectively. The results indicate that this hybrid electrode exhibits a high areal capacitance (52.55 mF cm^{-2}) that is 5 times higher than that of the control sample, which can be attributed to the elastic gel-wrapping effect.

2. EXPERIMENTAL SECTION

2.1. Materials. For the preparation of the agarose gel-coated substrate, a 1% (w/v) solution of agarose powder in deionized (DI) water was heated using a microwave oven. After the complete dissolution of the agarose, the solution was cast on a stainless steel (SS) plate (1 cm^2 circle) by a dip-coating method, and the agarose solution was allowed to form a gel on the plate at room temperature for 4 h in a sealed container. The Mn precursor solution for electrodeposition was prepared by dissolving 0.1 M of $Mn(NO_3)_2$ and 0.1 M of $NaNO_3$ in the DI water. The electrodeposition was performed potentiostatically at 1.2 V (vs Ag/AgCl) for various periods of time (10–1500 s). A saturated Ag/AgCl and a platinum plate were used as the reference and counter electrode, respectively. After electrodeposition, the deposited films were washed with DI water and dried at room temperature for 24 h.

2.2. Characterization. The surface morphology and composition of the prepared films were characterized by scanning electron microscopy (SEM, Carl Zeiss, SUPRA 55 VP) and focused-ion beam microscopy (FIB, Carl Zeiss, AURIGA). For the electrochemical measurements, cyclic voltammetry (CV) was performed in a standard three-electrode configuration (Iviumstat electrochemical analyzer, Ivium Technology) with an aqueous 1.0 M Na_2SO_4 solution as electrolyte. Electrochemical impedance spectroscopy (EIS) was conducted at an applied potential of 0.4 V, an ac amplitude of 10 mV, and frequencies of 100 mHz to 100 kHz. We used a saturated Ag/AgCl as the reference electrode and platinum counter electrode. The N_2 adsorption–desorption isotherms were recorded on a Micrometrics ASAP-2010 system to analyze pore structure and Brunauer–Emmett–Teller (BET) surface area of the film. The X-ray diffraction (XRD) patterns were obtained in 20–80° using X-ray diffractometer (Rigaku, D-MAX2500-PC). The 3D FEM simulation for the numerical

dx.doi.org/10.1021/am403532m | ACS Appl. Mater. Interfaces 2013, 5, 9908–9912

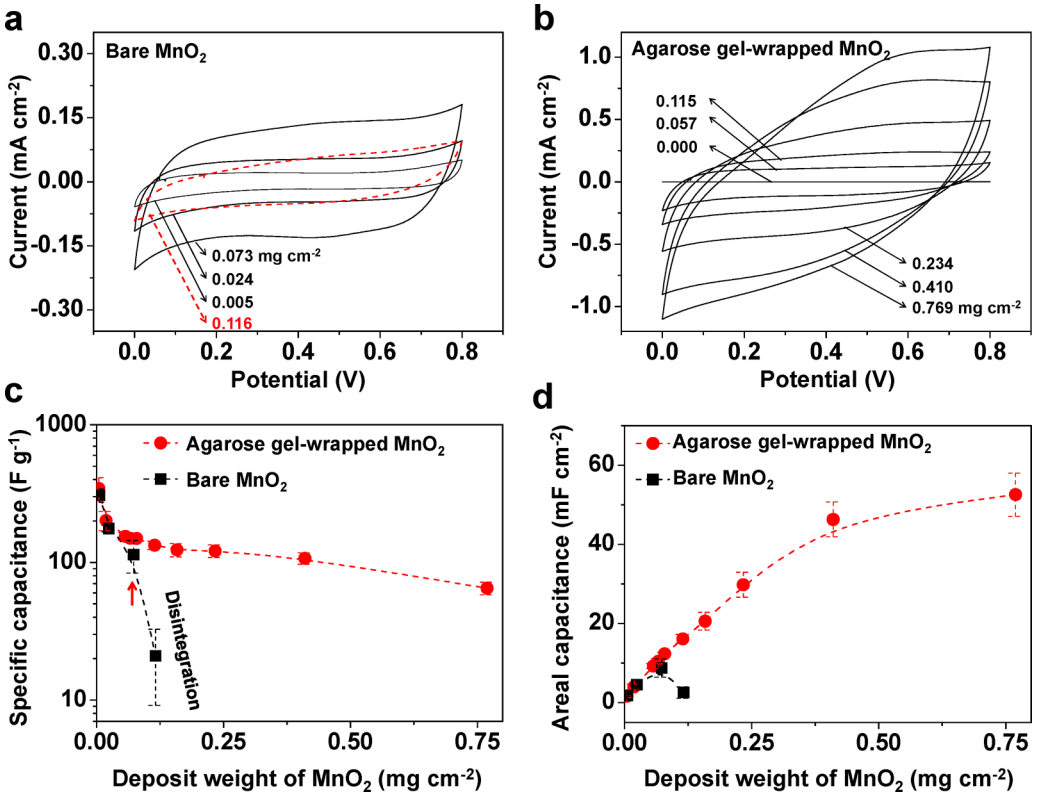

Figure 3. Cyclic voltammetry (CVs) results for (a) bare MnO_2 electrodes and (b) an agarose gel-wrapped MnO_2 electrode under different loading conditions. (c) Specific capacitance and (d) areal capacitance of electrode as a function of deposition weight of MnO_2.

structure analysis of agarose gel and the first principle calculation based on density functional theory (DFT) were performed. Details of these calculations can be found in the Supporting Information.

3. RESULTS AND DISCUSSION

Figure 1a shows schematic illustrations of the agarose gel-wrapped (AGW) MnO_2 films that were prepared by electrodeposition. Agarose gels, coated on the SS plate, function as a precoated and elastic wrapping layer for the deposited MnO_2. During the anodic electrodeposition, Mn^{2+} ions readily migrate through the gel layer, because the hydrophilicity and porous properties of the framework provide sufficient accessibility of the Mn^{2+} to current collector (SS). The electrodeposited MnO_2 films showed porous structure with BET surface area of 255.33 $m^2\ g^{-1}$ and crystalline structure containing γ-MnO_2 phase as proved in Figures S2 and S3 in the Supporting Information.

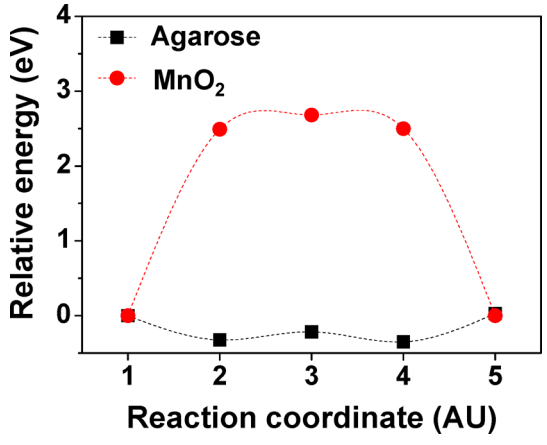

Figure 4. DFT calculated energy profile along the proton migration paths. The calculated total energies at each position of proton relative to the initial position are shown in *y*-axis.

As shown in Figure 1b and Figure S4 in the Supporting Information, in the absence of an agarose gel layer, the deposited MnO_2 films lose their structural rigidity, consequently becoming fragmented and separated from the current collector. In contrast, in the presence of an agarose gel layer, no cracks or isolations were observed (Figure 1c) when the same weight of MnO_2 was deposited. As indicated by panels a and d in Figure 1, the MnO_2 film that was grown on the current collector is enclosed within the agarose gel layer, resulting in three-layered structure (agarose gel/MnO_2/SS). The hierarchical structures of MnO_2 form as it is pushing up the gel layer and the elastic recovery force of the gel is exerted in the opposite direction (Figure 1e–g).

A 3D FEM simulation was performed to prove that the agarose gel has abundant elastic properties and it maintained in a hybridized form, even at high MnO_2 loadings. As shown in Figure 2a, we assumed that the gel is tensile-deformed along the *Z*-direction by about ~1.8 μm on the basis of previous SEM data. The maximum elastic strain and stress in such a deformation were calculated to be 2.6×10^{-7} μm/μm and 3.0×10^{-2} Pa, respectively (Figure 2b, c). The value for equivalent stress is very low, compared to the reported failure stress of the gel (48 KPa), indicating that the agarose gel completely encloses the deposited MnO_2 film due to its high elasticity.[15]

Based on the above findings, it can be concluded that the agarose gel effectively prevents the MnO_2 film from

dx.doi.org/10.1021/am403532m | ACS Appl. Mater. Interfaces 2013, 5, 9908–9912

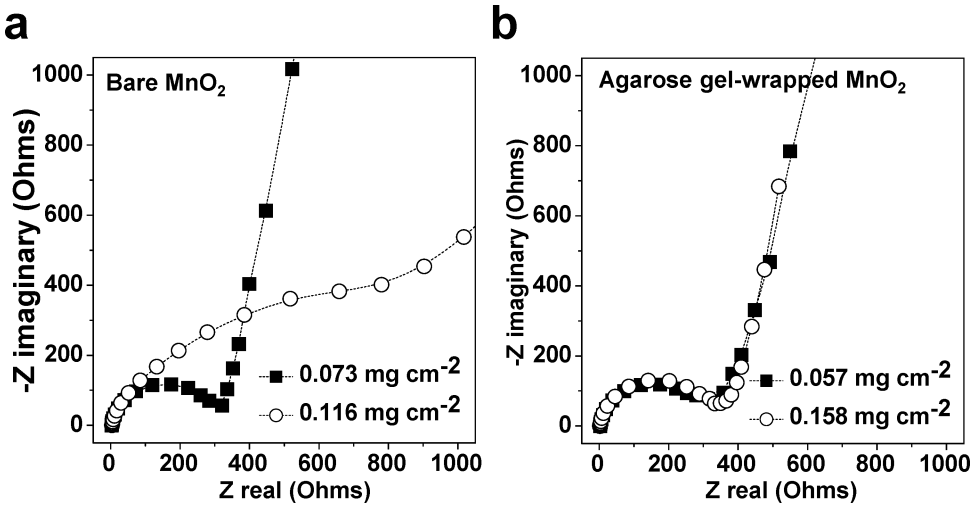

Figure 5. Nyquist impedance plots for (a) a bare MnO_2 electrode and (b) an agarose gel-wrapped MnO_2 electrode.

disintegrating and plays a key role in the formation of a robust MnO_2 film by virtue of its supportive and elastic properties. As a result, the agarose gel-wrapping permits intimate contact to be achieved between the MnO_2 film and the current collector. The improved stability of MnO_2 film by agarose gel-wrapping is visually shown in the Supporting Information, Movie S1.

The electrochemical properties and resistive behavior of the prepared AGW MnO_2 supercapacitor electrodes were evaluated by means of cyclic voltammetry and impedance spectroscopy measurements. These analyses were performed in the potential window from 0 to 0.8 V.

The CVs curves for the AGW MnO_2 films with various weights of deposited MnO_2 (~0.769 mg cm^{-2}) are summarized in Figure 3a, b. The deposited MnO_2 was quantified by measuring the accumulation capacity (mAh) during electrodeposition and the results show a linear correlation ($R^2 = 0.99$) between the measured accumulation capacity (mA h) and the weight of the deposited MnO_2 (see Figure S5 in the Supporting Information).[12] All CV curves were obtained at a scan rate of 10 mV s^{-1} and show a symmetrical and rectangular shape, indicative of good capacitance properties. Understandably, when the electroactive MnO_2 loading is increased, the overall capacitance of the electrode is also improved. In Figure 3a, the capacitance of a bare MnO_2 film was increased with increasing amounts of deposited MnO_2 up to a level of 0.073 mg cm^{-2}. When the amount of deposited MnO_2 reached 0.116 mg cm^{-2}; however, the capacitance of the electrode abruptly decreased. This result can be rationalized by assuming that there is a certain threshold regarding loading capacity (g cm^{-2}) for stable charge transfer and energy storage. MnO_2-deposited films over the threshold (0.073–0.116 mg cm^{-2}) become fragile and the initially deposited form of the film can no longer be retained (Figure 1b). To the contrary, AGW MnO_2 films show a consistent increase in capacitance even at relatively high MnO_2 loading levels (up to 0.769 mg cm^{-2}).

For a clear comparison between bare MnO_2 and AGW MnO_2, the values for specific capacitance (F g^{-1}) and areal capacitance (mF cm^{-2}) are plotted as a function of deposition weight in panels c and d in Figure 3. Under the low loading conditions employed (below 0.02 mg), both bare MnO_2 and AGW MnO_2 showed high capacitance values of 200–400 F g^{-1}, the level of which is similar to that found in literature reports.[1,6,20] However, the specific capacitances of a bare MnO_2 film sharply decreased when the deposition weight exceeded the threshold (indicated by the arrow) such that a value of 20.90 F g^{-1} was found when MnO_2 was deposited at a level of 0.116 mg cm^{-2}. Importantly, the MnO_2 inside the agarose gel films maintained its superior specific capacitance in the vicinity of 100 F g^{-1} up to 0.75 mg cm^{-2} (121.16 F g^{-1} at 0.23 mg cm^{-2}, 107.21 F g^{-1} at 0.41 mg cm^{-2}, and 64.92 F g^{-1} at 0.75 mg cm^{-2}). In Figure 3d, although the maximum areal capacitance of bare MnO_2 was 8.74 mF cm^{-2}, we were able to achieve a level of 52.55 mF cm^{-2} by taking advantage of the agarose gel-wrapping effect. The areal capacitance increased linearly up to 46.30 mF cm^{-2} with increasing amount of deposited MnO_2 increased (~0.41 mg cm^{-2}). This value for the areal capacitance surpasses previously reported results regarding the pseudocapacitive performance of electrodeposited MnO_2.[20−22] The rate capability of the AGW MnO_2 was investigated at various rates from 10 to 1000 mV s^{-1} because a fast charge−discharge can adversely affect the structural stability of the film (see Figure S6 in the Supporting Information). Importantly, when the rate returns to the initial 10 mV s^{-1} after 30 cycles, the AGW MnO_2 recovers its original capacitance (107.21 F g^{-1} at 0.41 mg cm^{-2}). In addition, no evidence of capacitance fading was found for AGW MnO_2 electrodes with a deposition weight of 0.77 mg cm^{-2} after 5000 cycles (within 10% of the initial capacitance) (see Figure S7 in the Supporting Information).

We conducted DFT calculations to predict the accessibility of electrolyte to the agarose gel-wrapped MnO_2. According to the previous reports regarding the charge storage mechanism of MnO_2, the pseudocapacitance of MnO_2 depends on the migration of protons into and out of the MnO_2 lattice under applied electrical fields.[23] When MnO_2 is reduced to produce MnOOH, protons are incorporated into the MnO_2 lattice. Based on this fundamental knowledge, we calculated and compared the energy required for proton migration through an agarose gel and a MnO_2 structure. Figure 4 shows the calculated relative energy at each point of the path, and indicates that the potential energy barrier for proton migration through the MnO_2 lattice is much larger than that for the migration of a proton through the agarose film (see details in Supporting Information). Therefore, the agarose gel is not the main obstacle to proton migration. Consequently, the loss of performance caused by agarose gel-wrapping can be negligible.

This excellent ion penetrability of agarose gels is also attributed to their large number of pores.

The Nyquist impedance plots for both electrodes (Figure 5) are very similar to both bare MnO_2 and AGW MnO_2 under conditions in which small amounts of MnO_2 were deposited. This result indicates that the resistive behavior of both electrodes are nearly identical, which are consistent with the DFT calculations. However, when the amount of deposited MnO_2 is increased to 0.116 mg cm^{-2}, the charge transfer resistance (Rct) in bare MnO_2 is dramatically increased. These results are in agreement with the drop in the capacitances of electrodes in the above-mentioned CVs (Figure 3a). In contrast, AGW MnO_2 maintained an equivalent Rct at a deposition weight of both 0.057 and 0.158 mg cm^{-2} (Figure 5b). This clearly demonstrates that the substrate adhesiveness of the agarose gel film plays a significant role in retaining the initially deposited forms of a MnO_2 layer without any loss electrical connectivity at the MnO_2/SS interface.

4. CONCLUSION

In conclusion, a facile synthesis of a robust metal oxide thin film involving agarose gel-mediated electrodeposition is reported. To prove our concept, we introduced an organic layer on the MnO_2 film by taking advantage of the inherent characteristics of agarose gels, including film-forming, ion-penetrable, and elastic properties, to achieve a high-performance pseudocapacitive electrode. The resulting electrode exhibited, not only an enhanced areal loading capacity, but a high utilization rate of MnO_2 as well. These improvements can be explained by a robust film structure and excellent contact with the metallic current collector. This study provides an effective route for organic-metal oxide hybridization by simply adding an agarose gel dip-coating procedure prior to the electrodeposition process.

■ ASSOCIATED CONTENT

Ⓢ Supporting Information

The calculation and computation details, the XRD pattern and SEM images of MnO_2 film, the quantification of deposited MnO_2, and the results of rate capability and long cycle test. This material is available free of charge via the Internet at http://pubs.acs.org.

■ AUTHOR INFORMATION

Corresponding Author

*E-mail: jyi@snu.ac.kr. Tel: +82-2-880-7438.

Notes

The authors declare no competing financial interest.

■ ACKNOWLEDGMENTS

This research was supported by WCU (World Class University) program through the National Research Foundation of Korea funded by the Ministry of Education, Science and Technology (R31-10013). This work also supported by the Energy Efficiency & Resources of the Korea Institute of Energy Technology Evaluation and Planning (KETEP) funded by the Korea government Ministry of Knowledge Economy (2012T100100511).

■ REFERENCES

(1) Nam, I.; Park, S.; Kim, G.-P.; Park, J.; Yi, J. *Chem. Sci.* **2013**, *4*, 1663−1667.
(2) Chen, P.-C.; Shen, G.; Sukcharoenchoke, S.; Zhou, C. *Appl. Phys. Lett.* **2009**, *94*, 043113.
(3) Yang, Y.; Jeong, S.; Hu, L.; Wu, H.; Lee, S. W.; Cui, Y. *Proc. Natl. Acad. Sci. U.S.A.* **2011**, *108*, 13013−13018.
(4) King, P. J.; Higgins, T. M.; De, S.; Nicoloso, N.; Coleman, J. N. *ACS Nano* **2012**, *6*, 1732−1741.
(5) Lee, S. W.; Gallant, B. M.; Byon, H. R.; Hammond, P. T.; Shao-Horn, Y. *Energy Environ. Sci.* **2011**, *4*, 1972−1985.
(6) Xia, H.; Lai, M. O.; Lu, L. *JOM* **2011**, *63*, 54−59.
(7) Wei, W.; Cui, X.; Chen, W.; Ivey, D. G. *Chem. Soc. Rev.* **2011**, *50*, 1697−1721.
(8) Wei, W.; Cui, X.; Chen, W.; Ivey, D. G. *J. Phys. Chem. C* **2008**, *112*, 15075−15083.
(9) Hu, C.-C.; Tsou, T.-W. *J. Power Sources* **2003**, *115*, 179−186.
(10) Nakayama, M.; Kanaya, T.; Inoue, R. *Electrochem. Commun.* **2007**, *9*, 1154−1158.
(11) Kim, G.-P.; Nam, I.; Kim, N. D.; Park, J.; Park, S.; Yi, J. *Electrochem. Commun.* **2012**, *22*, 93−96.
(12) Broughton, J. N.; Brett, M. J. *Electrochim. Acta* **2005**, *50*, 4814−4819.
(13) Nagarajan, N.; Humadi, H.; Zhitomirsky, I. *Electrochim. Acta* **2006**, *51*, 3039−3045.
(14) Pernodet, N.; Maaloum, M.; Tinland, B. *Electrophoresis* **1997**, *18*, 55−58.
(15) Normand, V.; Lootens, D. L.; Amici, E.; Plucknett, K. P.; Aymard, P. *Biomacromolecules* **2000**, *1*, 730−738.
(16) Shen, X.; Chen, X.; Liu, J.-H.; Huang, X.-J. *J. Mater. Chem.* **2009**, *19*, 7687−7693.
(17) Pluen, A.; Netti, P. A.; Jain, R. K.; Berk, D. A. *Biophys. J.* **1999**, *77*, 542−552.
(18) Park, S.; Nam, I.; Kim, G.-P.; Park, J.; Kim, N. D.; Kim, Y.; Yi, J. *Chem. Commun.* **2013**, *49*, 1554−1556.
(19) Kim, N. D.; Yun, H. J.; Nam, I.; Yi, J. *J. Mater. Chem.* **2011**, *21*, 15885−15888.
(20) Chou, S.; Cheng, F.; Chen, J. *J. Power Sources* **2006**, *162*, 727−734.
(21) Nam, I.; Kim, G.-P.; Park, S.; Park, J.; Kim, N. D.; Yi, J. *Nanoscale* **2012**, *4*, 7350−7353.
(22) Hu, C.-C.; Tsou, T.-W. *Electrochem. Commun.* **2002**, *4*, 105−109.
(23) Pang, S.-C.; Anderson, M. A.; Chapman, T. W. *J. Electrochem. Soc.* **2000**, *147*, 444−450.